

Error Analysis for the Euler Equations in Purely Algebraic Form

Volker Mehrmann* Jeroen J. Stolwijk*

May 18, 2015

Abstract

The presented work contains both a theoretical and a statistical error analysis for the Euler equations in purely algebraic form, also called the Weymouth equations or the temperature dependent algebraic model. These equations are obtained by performing several simplifications of the full Euler equations, which model the gas flow through a pipeline. The theoretical analysis is executed by first calculating the backward error and then the individual relative condition numbers. This error analysis results in a statement about the maximum pipeline length such that the algebraic model can be used safely. The statistical analysis is performed using both a Monte Carlo Simulation and the Univariate Reduced Quadrature Method and is used to illustrate and confirm the obtained theoretical results.

Keywords: error analysis, roundoff error, measurement error, condition number, backward error, statistical analysis

AMS subject classifications: 65G50, 65G30

*Institut für Mathematik, MA 4-5, TU Berlin, Strasse des 17. Juni 136, D-10623 Berlin, Germany.
{mehrmann, stolwijk}@math.tu-berlin.de

Contents

Symbols	3
Abbreviations	5
1 Introduction	6
1.1 Model Hierarchy	6
1.2 Sources of Uncertainty	8
1.3 Error Analysis and Conditioning	9
2 Error Analysis for the Algebraic Model	11
2.1 Theoretical Analysis	12
2.1.1 Mass Flux	12
2.1.2 Pressure	13
2.1.3 Temperature	16
2.2 Statistical Analysis	20
2.2.1 Monte Carlo Simulation	20
2.2.2 URQ Method	21
2.3 Simplification from Temperature Dependent to Isothermal Algebraic Model	24
3 Conclusion	26
Acknowledgements	26
References	27

Symbols

c_v	volumetric heat capacity
D	diameter of the pipeline
e	internal energy
E_{abs}	absolute error
E_{rel}	relative error
\mathbf{f}	output parameters
f_1	mass flux
g	gravitational constant
h	height above sea level
h'	slope of the pipeline
k_w	heat conductivity coefficient
L	pipeline length
λ	pipe friction coefficient
μ	mean of a random variable
N	sample size
n	number of input parameters
p	pressure
p_c	pseudocritical pressure
p_{in}	inlet pressure
\mathbf{q}	input parameters
R	gas constant
ρ	density
ρ_{in}	inlet density

σ	standard deviation of a random variable
T	temperature
T_c	pseudocritical temperature
t	time
T_{in}	inlet temperature
T_w	pipeline wall temperature
u	rounding unit
v	velocity
v_{in}	inlet velocity
x	coordinate along the pipeline
x_0	begin point of the pipeline
z	compressibility factor

Abbreviations

Eq.	Equation
Eqs.	Equations
h.o.t	higher order terms
i.e.	id est (<i>Latin</i>), that is
km	kilometre
MCS	Monte Carlo Simulation
ODE	Ordinary Differential Equation
PDE	Partial Differential Equation
rsd	relative standard deviation
Sec.	Section
URQ	Univariate Reduced Quadrature

1 Introduction

Gas plays a crucial role in the energy supply of Europe and the world. It is sufficiently and readily available, is traded, and is storable. After oil, natural gas is the second most used energy supplier in Germany, with a total share of 22.3% of the energy consumption in 2013 [6]. The large European pipeline network that is used for the transportation of natural gas is depicted in Fig. 1. The high and probably increasing demand for gas calls for a mathematical modeling, simulation, and optimisation of the gas transport through the pipeline network.

1.1 Model Hierarchy

In this work the gas flow through a pipeline is considered as a one-dimensional problem, where the variable x runs along the length of the pipe. This flow is modelled using the Euler equations, which are a system of nonlinear hyperbolic partial differential equations. It describes the behaviour of compressible, non viscous fluids and consists

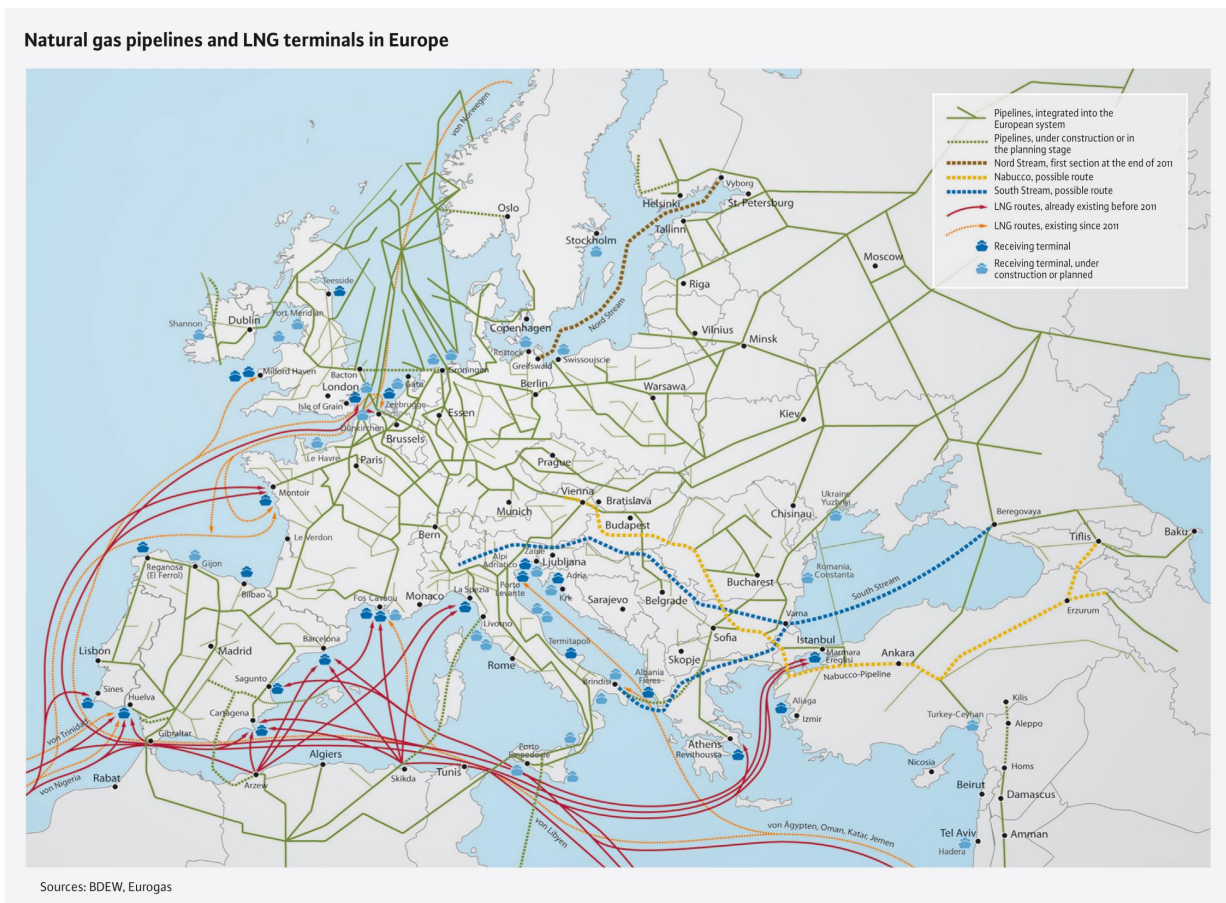


Fig. 1: Gas pipeline network in Europe [7].

of the continuity equation, the impulse equation, and the energy equation. The Euler equations are given by [10]

$$\begin{aligned} \frac{\partial \rho}{\partial t} + \frac{\partial}{\partial x}(\rho v) &= 0, \\ \frac{\partial}{\partial t}(\rho v) + \frac{\partial}{\partial x}(p + \rho v^2) &= -\frac{\lambda}{2D}\rho v|v| - g\rho h', \\ \frac{\partial}{\partial t}\left(\rho\left(\frac{1}{2}v^2 + e\right)\right) + \frac{\partial}{\partial x}\left(\rho v\left(\frac{1}{2}v^2 + e\right) + pv\right) &= -\frac{k_w}{D}(T - T_w). \end{aligned} \quad (1)$$

Moreover, the state equation for real gases, given by

$$p = R\rho T z(p, T),$$

holds. The variables have the following physical meaning (in the order of appearance):

- ρ = density of the gas,
- t = time,
- v = velocity of the gas,
- x = coordinate along the pipeline,
- p = pressure of the gas,
- λ = pipe friction coefficient,
- D = diameter of the pipeline,
- g = gravitational constant,
- h' = $h'(x)$ slope of the pipeline,
- e = $c_v T + gh$ internal energy (thermal + potential energy),
- c_v = volumetric heat capacity,
- T = temperature of the gas,
- h = height of the pipeline,
- k_w = heat conductivity coefficient,
- T_w = pipeline wall temperature,
- R = gas constant,
- z = $z(p, T)$ compressibility factor.

The full Euler equations in the one-dimensional case (1) are mathematically involved and their numerical solution requires much computational effort. For this reason, often several simplifications are made, which include the neglect of the terms $\frac{\partial}{\partial x}(\rho v^2)$, $\frac{\partial}{\partial x}(\rho v^3)$, and $\frac{\partial}{\partial t}(\rho v)$. Neglecting these three terms results in the model (ET3) in [2]

$$\begin{aligned} \frac{\partial \rho}{\partial t} + \frac{\partial}{\partial x}(\rho v) &= 0, \\ \frac{\partial p}{\partial x} &= -\frac{\lambda}{2D}\rho v|v| - g\rho h', \\ \frac{\partial}{\partial t}(\rho e) + \frac{\partial}{\partial x}(\rho v e + pv) &= -\frac{k_w}{D}(T - T_w), \end{aligned} \quad (2)$$

although the gravity is neglected in the asymptotic analysis of [2]. If then a stationary model is assumed, i.e., the time-derivatives $\frac{\partial}{\partial t}$ are set to zero, the gravity is neglected, and the compressibility factor z is set to be constant, the algebraic model in [5] is attained for the continuity and the impulse equations:

$$f_1 = \rho_{in} v_{in}, \quad (3)$$

$$p(x) = \sqrt{p_{in}^2 - \frac{\lambda c^2}{2D} \rho v |\rho v| (x - x_0)}, \quad (4)$$

where the constant $f_1 = \rho v$ is the mass flux, ρ_{in} is the inlet density, v_{in} is the inlet velocity, p_{in} is the inlet pressure, c is the constant speed of sound, and x_0 is the starting point of the pipeline. These assumptions reduce the energy equation to

$$\frac{\partial T}{\partial x} = -\frac{k_w}{D c_v \rho v} (T - T_w),$$

which can be analytically solved via

$$T(x) = (T_{in} - T_w) e^{-\frac{k_w}{D c_v \rho v} (x - x_0)} + T_w, \quad (5)$$

where T_{in} is the inlet temperature. The three Eqs. (3), (4), and (5), are referred to as the *temperature dependent algebraic model*. Another simplification can be made by taking the temperature T constant. This leaves us with the two Eqs. (3) and (4), which are referred to as the *isothermal algebraic model*.

1.2 Sources of Uncertainty

In mathematical models there are many sources of uncertainty and errors. First of all, a mathematical model is always a simplification of reality, such that a modeling error is made. Within a model, there are three main sources of errors in the numerical computation: rounding, data uncertainty, and truncation [8].

Rounding errors are unavoidable when one works in finite precision arithmetic on a computer. Rounding causes large errors for example in case of cancellation, i.e., when two approximately equal numbers are subtracted. Rounding errors are present in every single operation in an algorithm.

One should always be aware of uncertainties in the data when solving practical problems. Namely, measurement errors for physical quantities have been made. Also, rounding errors occur in storing the data on a computer. The effect of errors in the data are in general easier to understand than rounding errors in the computations, because data errors can be analysed using perturbation theory for the given problem, while intermediate rounding errors require an analysis specific to the given method or algorithm [8].

Truncation errors usually show up in the discretization of Ordinary Differential Equations (ODEs) and Partial Differential Equations (PDEs). Numerical integration methods can be derived by taking finitely many terms of a Taylor series. The truncation error is given by the omitted terms and depends on the stepsize.

1.3 Error Analysis and Conditioning

The aim of *error analysis* is to investigate the influence that all the different error sources in Sec. 1.2 have on the resulting solution. To what degree are the errors amplified in the solution? It tries to construct an a priori upper bound of the effects of the errors on the given problem and algorithm. Ideally, the upper bound is small for all choices of problem data [8]. If, however, the upper bound is large due to the rounding errors in the algorithm, we call it an *unstable* algorithm. This can be cured by choosing a different algorithm, if possible. If the upper bound is large due to the amplification of measurement errors in the given problem, we call it an *ill-conditioned*, unstable or ill-posed problem [12]. It indicates that the model may provide dubious results, which can only be cured by choosing a different model.

Important roles in the error analysis play the concepts of the *forward error*, the *backward error*, and the *condition number* or stability constant. The forward error is the difference between the exact solution of a mathematical problem $f(q)$ and the computed solution of the problem $\tilde{f}(q)$, including all the occurring errors. The backward error is given by that Δq for which $\tilde{f}(q) = f(q + \Delta q)$ holds, i.e., the occurring errors are interpreted as perturbations in the input parameter(s), such that the computed solution is the exact solution for perturbed data [1].

The word *condition* is used to describe the sensitivity of problems to uncertainties in the input parameters [12]. Suppose that the solution of a problem is obtained by evaluating the function of a single variable $f(q)$. Then, if the parameter q is changed to $q + \Delta q$, the solution $f(q)$ is changed to $f(q + \Delta q)$. Assuming that f is twice continuously differentiable, then the change in the solution is given by [8]

$$f(q + \Delta q) - f(q) = f'(q)\Delta q + \frac{f''(q + \theta\Delta q)}{2}(\Delta q)^2, \quad \theta \in (0, 1),$$

and the relative change in the solution is given by

$$\frac{f(q + \Delta q) - f(q)}{f(q)} = \left(\frac{qf'(q)}{f(q)} \right) \frac{\Delta q}{q} + O((\Delta q)^2). \quad (6)$$

The quantity

$$\kappa(q) = \left| \frac{qf'(q)}{f(q)} \right|,$$

with $|\cdot|$ the absolute value, is the *relative condition number* of f and it measures, for small Δq , the relative change in the output for a given relative change in the input. If, on the other hand, the solution of a problem is obtained by evaluating a function of several variables $f(\mathbf{q})$, the change in the solution due to perturbations in the input parameters $\mathbf{q} \in \mathbb{R}^n$ is given by

$$f(\mathbf{q} + \Delta \mathbf{q}) - f(\mathbf{q}) = \frac{\partial f}{\partial q_1} \Delta q_1 + \frac{\partial f}{\partial q_2} \Delta q_2 + \dots + \frac{\partial f}{\partial q_n} \Delta q_n + O((\Delta \mathbf{q})^2)$$

and the relative change in the solution is given by

$$\frac{f(\mathbf{q} + \Delta \mathbf{q}) - f(\mathbf{q})}{f(\mathbf{q})} = \left(\frac{\partial f}{\partial q_1} \frac{q_1}{f(\mathbf{q})} \right) \frac{\Delta q_1}{q_1} + \dots + \left(\frac{\partial f}{\partial q_n} \frac{q_n}{f(\mathbf{q})} \right) \frac{\Delta q_n}{q_n} + O((\Delta \mathbf{q})^2). \quad (7)$$

The quantities

$$\kappa_{q_i}(\mathbf{q}) = \left| \frac{\partial f}{\partial q_i} \frac{q_i}{f(\mathbf{q})} \right|, \quad i = 1, \dots, n, \quad (8)$$

are the *individual relative condition numbers* with respect to q_i [9]. Furthermore, the vector

$$\boldsymbol{\kappa}(\mathbf{q}) = [\kappa_{q_1}(\mathbf{q}), \dots, \kappa_{q_n}(\mathbf{q})] \in \mathbb{R}_+^{1 \times n} \quad (9)$$

is the *vector relative condition number* and the quantity

$$\kappa_p^*(q) = \|\boldsymbol{\kappa}(q)\|_p$$

is the *overall relative condition number* with respect to the p -norm. If the quantity $\kappa_p^*(q)$ is small, the problem is called *well-conditioned*, and if $\kappa_p^*(q)$ is large, the problem is called *ill-conditioned*. The size of $\kappa_p^*(q)$ is measured in the context of the rounding unit \mathbf{u} . Usually, the problem is considered as very well-conditioned if $\kappa_p^*(q) \approx 1$ and as very ill-conditioned if $\mathbf{u} \kappa_p^*(q) \approx 1$, [9].

The relation between the forward error, the backward error, and the condition number can be nicely seen from Eq. (6). Taking the absolute value of the relative change in the solution gives

$$\left| \frac{f(q + \Delta q) - f(q)}{f(q)} \right| \leq \kappa(q) \left| \frac{\Delta q}{q} \right| + O((\Delta q)^2),$$

such that we have the following rule of thumb:

$$\text{forward error} \lesssim \text{condition number} \times \text{backward error},$$

with \lesssim meaning "approximately less than". It insightfully shows that despite of a small backward error, a problem can have a large forward error due to a high condition number.

2 Error Analysis for the Algebraic Model

In this chapter an error analysis is performed on the temperature dependent algebraic model in Eqs. (3), (4), and (5). The Euler equations in algebraic form, also called the Weymouth equations, are given by

$$\begin{aligned} \mathbf{f}(\mathbf{q}) &= \mathbf{f}(\rho_{in}, v_{in}, \rho, v, p_{in}, \lambda, c, D, x, x_0, T_{in}, T_w, k_w, c_v) \\ &= \begin{bmatrix} \rho_{in} v_{in} \\ \sqrt{p_{in}^2 - \frac{\lambda c^2}{2D} \rho v} | \rho v | (x - x_0) \\ (T_{in} - T_w) e^{-\frac{k_w}{D c_v \rho v} (x - x_0)} + T_w \end{bmatrix} = \begin{bmatrix} f_1(\mathbf{q}) \\ p(\mathbf{q}) \\ T(\mathbf{q}) \end{bmatrix}, \end{aligned} \quad (10)$$

where the physical meaning of the parameters is given in Sec. 1.1 and in the List of Symbols. A concise derivation of these equations is given in Sec. 1.1 and for the isothermal algebraic model in [4]. The Jacobian matrix $J_f(\mathbf{q})$ of $\mathbf{f}(\mathbf{q})$ is given by

$$J_f(\mathbf{q}) = \begin{bmatrix} \frac{\partial f_1}{\partial \rho_{in}} & \frac{\partial p}{\partial \rho_{in}} & \frac{\partial T}{\partial \rho_{in}} \\ \frac{\partial f_1}{\partial v_{in}} & \frac{\partial p}{\partial v_{in}} & \frac{\partial T}{\partial v_{in}} \\ \frac{\partial f_1}{\partial \rho} & \frac{\partial p}{\partial \rho} & \frac{\partial T}{\partial \rho} \\ \frac{\partial f_1}{\partial v} & \frac{\partial p}{\partial v} & \frac{\partial T}{\partial v} \\ \frac{\partial f_1}{\partial p_{in}} & \frac{\partial p}{\partial p_{in}} & \frac{\partial T}{\partial p_{in}} \\ \frac{\partial f_1}{\partial \lambda} & \frac{\partial p}{\partial \lambda} & \frac{\partial T}{\partial \lambda} \\ \frac{\partial f_1}{\partial c} & \frac{\partial p}{\partial c} & \frac{\partial T}{\partial c} \\ \frac{\partial f_1}{\partial D} & \frac{\partial p}{\partial D} & \frac{\partial T}{\partial D} \\ \frac{\partial f_1}{\partial x} & \frac{\partial p}{\partial x} & \frac{\partial T}{\partial x} \\ \frac{\partial f_1}{\partial x_0} & \frac{\partial p}{\partial x_0} & \frac{\partial T}{\partial x_0} \\ \frac{\partial f_1}{\partial T_{in}} & \frac{\partial p}{\partial T_{in}} & \frac{\partial T}{\partial T_{in}} \\ \frac{\partial f_1}{\partial T_w} & \frac{\partial p}{\partial T_w} & \frac{\partial T}{\partial T_w} \\ \frac{\partial f_1}{\partial k_w} & \frac{\partial p}{\partial k_w} & \frac{\partial T}{\partial k_w} \\ \frac{\partial f_1}{\partial c_v} & \frac{\partial p}{\partial c_v} & \frac{\partial T}{\partial c_v} \end{bmatrix}^T = \begin{bmatrix} v_{in} & 0 & 0 \\ \rho_{in} & 0 & 0 \\ 0 & -\frac{\rho \lambda c^2 v^2 (x - x_0)}{2Dp(x)} & \frac{(T_{in} - T_w) k_w (x - x_0)}{D c_v \rho^2 v} e^{-\frac{k_w (x - x_0)}{D c_v \rho v}} \\ 0 & -\frac{v \lambda c^2 \rho^2 (x - x_0)}{2Dp(x)} & \frac{(T_{in} - T_w) k_w (x - x_0)}{D c_v \rho v^2} e^{-\frac{k_w (x - x_0)}{D c_v \rho v}} \\ 0 & \frac{p_{in}}{p(x)} & 0 \\ 0 & -\frac{c^2 \rho^2 v^2 (x - x_0)}{4Dp(x)} & 0 \\ 0 & -\frac{c \lambda v^2 \rho^2 (x - x_0)}{2Dp(x)} & 0 \\ 0 & \frac{\lambda c^2 \rho^2 v^2 (x - x_0)}{4D^2 p(x)} & \frac{(T_{in} - T_w) k_w (x - x_0)}{D^2 c_v \rho v} e^{-\frac{k_w (x - x_0)}{D c_v \rho v}} \\ 0 & -\frac{\lambda c^2 \rho^2 v^2}{4Dp(x)} & -\frac{(T_{in} - T_w) k_w}{D c_v \rho v} e^{-\frac{k_w (x - x_0)}{D c_v \rho v}} \\ 0 & \frac{\lambda c^2 \rho^2 v^2}{4Dp(x)} & \frac{(T_{in} - T_w) k_w}{D c_v \rho v} e^{-\frac{k_w (x - x_0)}{D c_v \rho v}} \\ 0 & 0 & e^{-\frac{k_w (x - x_0)}{D c_v \rho v}} \\ 0 & 0 & 1 - e^{-\frac{k_w (x - x_0)}{D c_v \rho v}} \\ 0 & 0 & -\frac{(T_{in} - T_w) (x - x_0)}{D c_v \rho v} e^{-\frac{k_w (x - x_0)}{D c_v \rho v}} \\ 0 & 0 & \frac{(T_{in} - T_w) k_w (x - x_0)}{D c_v^2 \rho v} e^{-\frac{k_w (x - x_0)}{D c_v \rho v}} \end{bmatrix}^T,$$

which is used for the computation of the individual relative condition numbers, Eq. (8).

2.1 Theoretical Analysis

In this section the backward error is computed for the three equations in (10). The computational rounding errors due to finite precision arithmetic and measurement errors are interpreted as perturbations in the input parameters. Then, the relative errors in the output parameters are calculated and analysed.

2.1.1 Mass Flux

In the equation for the mass flux,

$$f_1(q) = \rho_{in} v_{in}, \quad (11)$$

only one multiplication is performed with relative error ε_1 , which yields

$$\begin{aligned} \tilde{f}_1(\rho_{in}, v_{in}) &= \rho_{in}(1 + \varepsilon_{\rho_{in}})v_{in}(1 + \varepsilon_{v_{in}})(1 + \varepsilon_1) \\ &= \rho_{in}v_{in}(1 + \varepsilon_{\rho_{in}} + \varepsilon_{v_{in}} + \varepsilon_1 + O(\varepsilon^2)) = f_1(\rho_{in}, v_{in}(1 + \varepsilon_2)), \end{aligned} \quad (12)$$

with $\varepsilon_2 = \varepsilon_{\rho_{in}} + \varepsilon_{v_{in}} + \varepsilon_1 + O(\varepsilon^2)$. Here, $\varepsilon_{\rho_{in}}$ is the relative measurement error in ρ_{in} , $\varepsilon_{v_{in}}$ the relative measurement error in v_{in} , and $|\varepsilon_1| < \mathbf{u}$ the relative error of the multiplication, with \mathbf{u} the rounding unit in finite precision arithmetic.

For the absolute relative error in f_1 , using Eq. (12), it holds that

$$\begin{aligned} \frac{|f_1(q) - f_1(q + \Delta q)|}{|f_1(q)|} &\leq \left| \frac{\partial f_1}{\partial \rho_{in}} \frac{1}{f_1(q)} \underbrace{\Delta \rho_{in}}_0 \right| + \left| \frac{\partial f_1}{\partial v_{in}} \frac{1}{f_1(q)} \Delta v_{in} \right| + O((\Delta q)^2) \\ &= \left| \underbrace{\left(\frac{\partial f_1}{\partial v_{in}} \frac{v_{in}}{f_1(q)} \right)}_{\frac{\rho_{in} v_{in}}{\rho_{in} v_{in}} = 1} \underbrace{\frac{\Delta v_{in}}{v_{in}}}_{\varepsilon_2} \right| + O((\Delta q)^2) \\ &= |\varepsilon_2| + \text{h.o.t.} \leq |\varepsilon_{\rho_{in}}| + |\varepsilon_{v_{in}}| + |\varepsilon_1| + \text{h.o.t.}, \end{aligned}$$

where h.o.t. stands for higher order terms, i.e., $O(\varepsilon^2)$. This means that if the relative error in f_1 has to stay below a certain limit e_{lim} , for example $e_{lim} = 0.1$, then the sum of the relative measurement errors $\varepsilon_{\rho_{in}}$ and $\varepsilon_{v_{in}}$ should stay below this limit e_{lim} . We assume that round-off error ε_1 is so small that it can be neglected in comparison with errors $\varepsilon_{\rho_{in}}$ and $\varepsilon_{v_{in}}$. Concluding, the constraint

$$|\varepsilon_{\rho_{in}}| + |\varepsilon_{v_{in}}| \lesssim e_{lim}, \quad (13)$$

except for h.o.t., is found.

2.1.2 Pressure

For computing the pressure

$$p(q) = \sqrt{p_{in}^2 - \frac{\lambda c^2}{2D} \rho v |\rho v| (x - x_0)}, \quad (14)$$

we can apply Algorithm 1. Using the Taylor expansion

$$\frac{1}{1 - \varepsilon} = 1 + \varepsilon + O(\varepsilon^2), \quad (15)$$

this leads to a backward error due to roundoff errors in finite precision arithmetic

$$\begin{aligned} \tilde{p}(q) &= \sqrt{p_{in}^2 (1 + \varepsilon_1)(1 + \varepsilon_{11}) - \frac{\lambda c^2 (1 + \varepsilon_2)(1 + \varepsilon_3)}{2D(1 - \varepsilon_4)} (1 + \varepsilon_5) \rho v (1 + \varepsilon_6)(1 + \varepsilon_8) |\rho v|} \\ &\quad \cdot \sqrt{(1 + \varepsilon_6)(1 + \varepsilon_9)(x - x_0)(1 + \varepsilon_7)(1 + \varepsilon_{10})(1 + \varepsilon_{11})(1 + \varepsilon_{12})} \\ &= \sqrt{(p_{in}(1 + \varepsilon_{13}))^2 - \frac{\lambda(1 + \varepsilon_{14})c^2}{2D} \rho v |\rho v| (x - x_0)}, \end{aligned} \quad (16)$$

where

$$2 \cdot |\varepsilon_{13}| = |\varepsilon_1 + \varepsilon_{11} + 2\varepsilon_{12} + O(\varepsilon^2)| \leq 4 \cdot \mathbf{u} + O(\mathbf{u}^2),$$

so that

$$|\varepsilon_{13}| \leq 2 \cdot \mathbf{u} + O(\mathbf{u}^2),$$

Algorithm 1 : Compute the pressure p , Eq. (14)

Input: $p_{in}, \lambda, c, D, \rho, v, x, x_0$

- 1: $z_1 \leftarrow p_{in} \cdot p_{in}$
- 2: $z_2 \leftarrow c \cdot c$
- 3: $z_3 \leftarrow \lambda \cdot z_2$
- 4: $z_4 \leftarrow 2 \cdot D$
- 5: $z_5 \leftarrow z_3 / z_4$
- 6: $z_6 \leftarrow \rho \cdot v$
- 7: $z_7 \leftarrow x - x_0$
- 8: $z_8 \leftarrow z_5 \cdot z_6$
- 9: $z_9 \leftarrow z_8 \cdot |z_6|$
- 10: $z_{10} \leftarrow z_9 \cdot z_7$
- 11: $z_{11} \leftarrow z_1 - z_{10}$
- 12: $z_{12} \leftarrow \sqrt{z_{11}}$
- 13: $p(q) \leftarrow z_{12}$

Output: p

and

$$\begin{aligned} |\varepsilon_{14}| &= |\varepsilon_2 + \varepsilon_3 + \varepsilon_4 + \varepsilon_5 + \varepsilon_6 + \varepsilon_8 + \varepsilon_6 + \varepsilon_9 + \varepsilon_7 + \varepsilon_{10} + \varepsilon_{11} + 2\varepsilon_{12} + O(\varepsilon^2)| \\ &\leq 13 \cdot \mathbf{u} + O(\mathbf{u}^2). \end{aligned}$$

As a next step, measurement errors are introduced for all parameters. For example, the measurement error for the parameter x is denoted by ε_x . Continuing with Eq. (16), this gives

$$\begin{aligned} \tilde{p}(q)^2 &= (p_{in}(1 + \varepsilon_{p_{in}})(1 + \varepsilon_{13}))^2 \\ &\quad - \frac{\lambda(1 + \varepsilon_\lambda)(1 + \varepsilon_{14})c^2(1 + \varepsilon_c)^2}{2D(1 - \varepsilon_D)} \rho v |\rho v| (1 + \varepsilon_\rho)^2 (1 + \varepsilon_v)^2 (x(1 + \varepsilon_x) - x_0(1 + \varepsilon_{x_0})) \\ &= (p_{in}(1 + \varepsilon_{15}))^2 - \frac{\lambda(1 + \varepsilon_{16})c^2}{2D} \rho v |\rho v| (x(1 + \varepsilon_x) - x_0(1 + \varepsilon_{x_0})), \end{aligned} \quad (17)$$

with

$$|\varepsilon_{15}| = |\varepsilon_{p_{in}} + \varepsilon_{13} + O(\varepsilon^2)| \leq |\varepsilon_{p_{in}}| + 2 \cdot \mathbf{u} + \text{h.o.t.}, \quad (18)$$

and

$$\begin{aligned} |\varepsilon_{16}| &= |\varepsilon_\lambda + \varepsilon_{14} + 2\varepsilon_c + \varepsilon_D + 2\varepsilon_\rho + 2\varepsilon_v + O(\varepsilon^2)| \\ &\leq |\varepsilon_\lambda| + 2 \cdot |\varepsilon_c| + |\varepsilon_D| + 2 \cdot |\varepsilon_\rho| + 2 \cdot |\varepsilon_v| + 13 \cdot \mathbf{u} + \text{h.o.t.} \end{aligned} \quad (19)$$

So for the backward error of $p(q)$, considered as a function of p_{in} , λ , x , and x_0 , we have the expression

$$\tilde{p}(p_{in}, \lambda, x, x_0) = p(p_{in}(1 + \varepsilon_{15}), \lambda(1 + \varepsilon_{16}), x(1 + \varepsilon_x), x_0(1 + \varepsilon_{x_0})).$$

Now that the backward error is obtained, the relative error in $p(q)$ due to perturbations in the data q can be calculated and is given by

$$\begin{aligned} \frac{p(q) - p(q + \Delta q)}{p(q)} &= \frac{\partial p(q)}{\partial p_{in}} \frac{p_{in}}{p(q)} \frac{\Delta p_{in}}{p_{in}} + \frac{\partial p(q)}{\partial \lambda} \frac{\lambda}{p(q)} \frac{\Delta \lambda}{\lambda} + \frac{\partial p(q)}{\partial x} \frac{x}{p(q)} \frac{\Delta x}{x} + \frac{\partial p(q)}{\partial x_0} \frac{x_0}{p(q)} \frac{\Delta x_0}{x_0} \\ &\quad + O((\Delta q)^2) \\ &= \underbrace{\left(\frac{p_{in}}{p(q)} \right)^2}_{\kappa_{p_{in}}(q)} \varepsilon_{15} - \underbrace{\frac{\lambda c^2 \rho^2 v^2 (x - x_0)}{4D p(q)^2}}_{\kappa_\lambda(q)} \varepsilon_{16} - \underbrace{\frac{\lambda c^2 \rho^2 v^2 x}{4D p(q)^2}}_{\kappa_x(q)} \varepsilon_x + \underbrace{\frac{\lambda c^2 \rho^2 v^2 x_0}{4D p(q)^2}}_{\kappa_{x_0}(q)} \varepsilon_{x_0} \\ &\quad + \text{h.o.t.}, \end{aligned}$$

where $\kappa_{p_{in}}$, κ_λ , κ_x , and κ_{x_0} are the individual relative condition numbers, Eq. (8). For the relative condition number $\kappa_{p_{in}}(q)$ with respect to p_{in} it holds that

$$\kappa_{p_{in}}(q) = \left(\frac{p_{in}}{p(q)} \right)^2 > 1,$$

because $p(q) = \sqrt{p_{in}^2 - \frac{\lambda c^2}{2D} \rho v |\rho v| (x - x_0)} < \sqrt{p_{in}^2} = p_{in}$. Taking the nominal values q_{nom} as

$$\begin{aligned} p_{in_{nom}} &= 2 \cdot 10^5 \text{ (or 2 bar)}, \\ \lambda_{nom} &= 0.06, \\ c_{nom} &= 343, \\ D_{nom} &= 1, \\ \rho_{nom} &= 1, \\ v_{nom} &= 10, \\ x_{nom} &= 10^5 \text{ (or 100 km), and} \\ x_{0_{nom}} &= 0, \end{aligned} \tag{20}$$

gives an amplification factor of

$$\kappa_{p_{in}}(q_{nom}) = 8.5.$$

For the relative condition number $\kappa_\lambda(q)$ it holds that $\kappa_\lambda \leq 1$ if and only if

$$L = x - x_0 \leq \frac{4Dp_{in}^2}{3\lambda c^2 \rho^2 v^2}.$$

Substituting the nominal values q_{nom} , Eq. (20), yields

$$L \leq 7.56 \cdot 10^4.$$

With nominal values q_{nom} in Eq. (20), in particular $x_{0_{nom}} = 0$, it holds that $\kappa_x(q) = \kappa_\lambda(q)$ and $\kappa_{x_0}(q) = 0$. The relative condition numbers $\kappa_{p_{in}}$ and κ_λ are given in Fig. 2 as a function of the pipeline length $L = x - x_0$. The remaining input parameters are fixed to the values in Eq. (20). This figure shows that the relative condition numbers grow quickly with increasing pipeline length L . The two graphs have a vertical asymptote at $L \approx 113$ km, as the pressure in this point is

$$p(q_{nom}, x = 113, 331) = 404 \text{ Pa}, \tag{21}$$

which is approximately zero.

It can be concluded that the algebraic model can only be used safely for pipelines up to 60 km length. For pipelines longer than 60 km the pressure can not be computed accurately as the relative condition number $\kappa_{p_{in}}$ is then larger than two. A more accurate model in the model hierarchy, see Sec. 1.1, should be chosen for the pipelines longer than 60 km.

2.1.3 Temperature

To compute the temperature

$$T(q) = (T_{in} - T_w)e^{-\frac{k_w}{Dc_v\rho v}(x-x_0)} + T_w, \quad (22)$$

Algorithm 2 can be applied. As every step introduces a relative error ε , the following

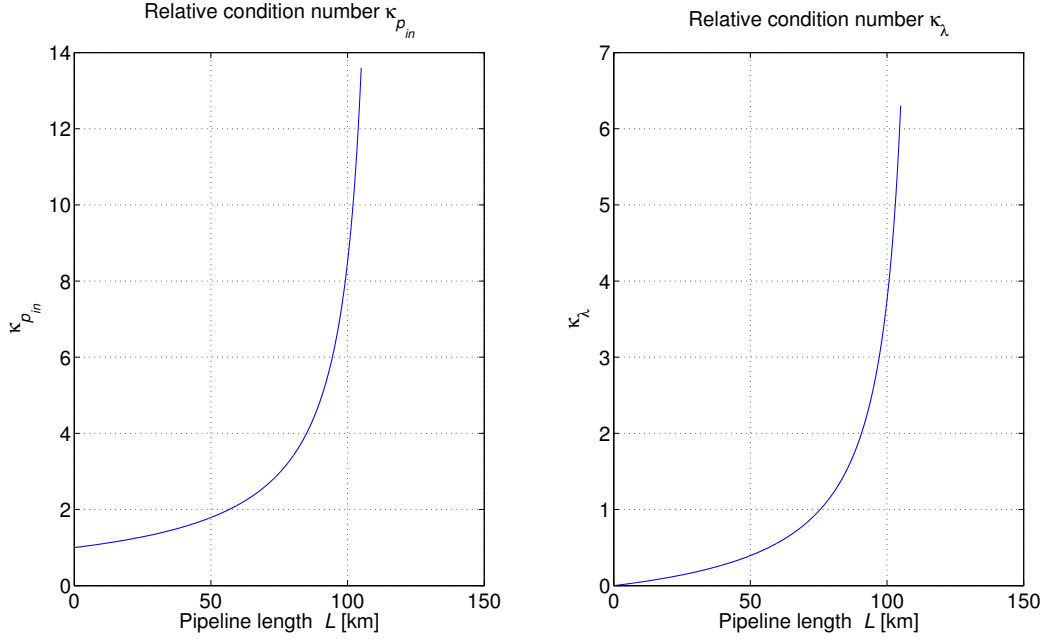


Fig. 2: Individual relative condition numbers $\kappa_{p_{in}}$ and κ_{λ} with respect to p_{in} and λ , respectively, for the pressure p , considered as a function of the pipeline length $L = x - x_0$.

Algorithm 2 : Compute the temperature T , Eq. (22)

Input: $T_{in}, T_w, k_w, D, c_v, \rho, v, x, x_0$

- 1: $z_1 \leftarrow T_{in} - T_w$
- 2: $z_2 \leftarrow D \cdot c_v$
- 3: $z_3 \leftarrow z_2 \cdot \rho$
- 4: $z_4 \leftarrow z_3 \cdot v$
- 5: $z_5 \leftarrow k_w / z_4$
- 6: $z_6 \leftarrow x - x_0$
- 7: $z_7 \leftarrow z_5 \cdot z_6$
- 8: $z_8 \leftarrow e^{-z_7}$
- 9: $z_9 \leftarrow z_1 \cdot z_8$
- 10: $z_{10} \leftarrow z_9 + T_w$
- 11: $T(q) \leftarrow z_{10}$

Output: T

expression is obtained, using the Taylor series expansion in Eq. (15),

$$\begin{aligned}
\tilde{T}(q) &= [(T_{in} - T_w)(1 + \varepsilon_1)e^{-\frac{k_w}{Dc_v(1-\varepsilon_2)\rho(1-\varepsilon_3)v(1-\varepsilon_4)}(1+\varepsilon_5)(x-x_0)(1+\varepsilon_6)(1+\varepsilon_7)}(1 + \varepsilon_8)(1 + \varepsilon_9) \\
&\quad + T_w](1 + \varepsilon_{10}) \\
&= (T_{in}(1 + \varepsilon_{11}) - T_w(1 + \varepsilon_{11}))e^{-\frac{k_w(1+\varepsilon_{12})}{Dc_v\rho v}(x-x_0)} + T_w(1 + \varepsilon_{10}) \\
&= \left(T_{in}(1 + \varepsilon_{11} - \frac{T_w}{T_{in}}(\varepsilon_{11} - \varepsilon_{10})) - T_w(1 + \varepsilon_{10})\right)e^{-\frac{k_w(1+\varepsilon_{12})}{Dc_v\rho v}(x-x_0)} + T_w(1 + \varepsilon_{10}),
\end{aligned} \tag{23}$$

where

$$\begin{aligned}
1 + \varepsilon_{11} &= (1 + \varepsilon_1)(1 + \varepsilon_8)(1 + \varepsilon_9)(1 + \varepsilon_{10}), \\
1 + \varepsilon_{12} &= (1 + \varepsilon_2)(1 + \varepsilon_3)(1 + \varepsilon_4)(1 + \varepsilon_5)(1 + \varepsilon_6)(1 + \varepsilon_7), \\
|\varepsilon_{10}| &\leq \mathbf{u}, \\
|\varepsilon_{11}| &= |\varepsilon_1 + \varepsilon_8 + \varepsilon_9 + \varepsilon_{10} + O(\varepsilon^2)| \leq 4\mathbf{u} + O(\mathbf{u}^2), \quad \text{and} \\
|\varepsilon_{12}| &= |\varepsilon_2 + \varepsilon_3 + \varepsilon_4 + \varepsilon_5 + \varepsilon_6 + \varepsilon_7 + O(\varepsilon^2)| \leq 6\mathbf{u} + O(\mathbf{u}^2).
\end{aligned}$$

This leads to a backward error for $T(q)$, considered as a function of T_{in} , T_w , and k_w , given by the expression

$$\tilde{T}(T_{in}, T_w, k_w) = T \left(T_{in}(1 + \varepsilon_{11} - \frac{T_w}{T_{in}}(\varepsilon_{11} - \varepsilon_{10})), T_w(1 + \varepsilon_{10}), k_w(1 + \varepsilon_{12}) \right).$$

Including measurement errors for the input parameters, continuing with Eq. (23), gives

$$\begin{aligned}
\tilde{T}(q) &= \left(T_{in}(1 + \varepsilon_{T_{in}})(1 + \varepsilon_{11} - \frac{T_w(1 + \varepsilon_{T_w})}{T_{in}(1 - \varepsilon_{T_{in}})}(\varepsilon_{11} - \varepsilon_{10})) - T_w(1 + \varepsilon_{T_w})(1 + \varepsilon_{10}) \right) \\
&\quad \cdot e^{-\frac{k_w(1+\varepsilon_{k_w})(1+\varepsilon_{12})}{D(1-\varepsilon_D)c_v(1-\varepsilon_{c_v})\rho(1-\varepsilon_\rho)v(1-\varepsilon_v)}(x(1+\varepsilon_x)-x_0(1+\varepsilon_{x_0}))} + T_w(1 + \varepsilon_{T_w})(1 + \varepsilon_{10}) \\
&= (T_{in}(1 + \varepsilon_{13}) - T_w(1 + \varepsilon_{14}))e^{-\frac{k_w(1+\varepsilon_{15})}{Dc_v\rho v}(x(1+\varepsilon_x)-x_0(1+\varepsilon_{x_0}))} + T_w(1 + \varepsilon_{14}),
\end{aligned}$$

where

$$\begin{aligned}
1 + \varepsilon_{13} &= (1 + \varepsilon_{T_{in}})(1 + \varepsilon_{11} - \frac{T_w(1 + \varepsilon_{T_w})}{T_{in}(1 - \varepsilon_{T_{in}})}(\varepsilon_{11} - \varepsilon_{10})) \\
&= 1 + \varepsilon_{T_{in}} + \varepsilon_{11} - \frac{T_w}{T_{in}}(\varepsilon_{11} - \varepsilon_{10}) + O(\varepsilon^2), \\
1 + \varepsilon_{14} &= (1 + \varepsilon_{T_w})(1 + \varepsilon_{10}) = 1 + \varepsilon_{T_w} + \varepsilon_{10} + O(\varepsilon^2), \quad \text{and} \\
1 + \varepsilon_{15} &= (1 + \varepsilon_{k_w})(1 + \varepsilon_{12})(1 + \varepsilon_D)(1 + \varepsilon_{c_v})(1 + \varepsilon_\rho)(1 + \varepsilon_v) + O(\varepsilon^2) \\
&= 1 + \varepsilon_{k_w} + \varepsilon_{12} + \varepsilon_D + \varepsilon_{c_v} + \varepsilon_\rho + \varepsilon_v + O(\varepsilon^2).
\end{aligned}$$

This results in the backward error

$$\tilde{T}(T_{in}, T_w, k_w, x, x_0) = T(T_{in}(1 + \varepsilon_{13}), T_w(1 + \varepsilon_{14}), k_w(1 + \varepsilon_{15}), x(1 + \varepsilon_x), x_0(1 + \varepsilon_{x_0})).$$

For the relative error in the temperature $T(q)$ due to finite precision arithmetic and data errors, it holds that

$$\begin{aligned} \frac{T(q) - \tilde{T}(q)}{T(q)} &= \frac{T(q) - T(q + \Delta q)}{T(q)} \\ &= \left(\frac{\partial T(q)}{\partial T_{in}} \frac{T_{in}}{T(q)} \right) \frac{\Delta T_{in}}{T_{in}} + \left(\frac{\partial T(q)}{\partial T_w} \frac{T_w}{T(q)} \right) \frac{\Delta T_w}{T_w} + \left(\frac{\partial T(q)}{\partial k_w} \frac{k_w}{T(q)} \right) \frac{\Delta k_w}{k_w} \\ &\quad + \left(\frac{\partial T(q)}{\partial x} \frac{x}{T(q)} \right) \frac{\Delta x}{x} + \left(\frac{\partial T(q)}{\partial x_0} \frac{x_0}{T(q)} \right) \frac{\Delta x_0}{x_0} + O((\Delta q)^2) \\ &= \underbrace{\frac{T_{in}}{T_{in} + \left(e^{\frac{k_w(x-x_0)}{Dc_v\rho v}} - 1 \right) T_w}}_{\kappa_{T_{in}}(q)} \varepsilon_{13} + \underbrace{\frac{T_w - T_w e^{-\frac{k_w(x-x_0)}{Dc_v\rho v}}}{(T_{in} - T_w) e^{-\frac{k_w(x-x_0)}{Dc_v\rho v}} + T_w}}_{\kappa_{T_w}(q)} \varepsilon_{14} \\ &\quad - \underbrace{\frac{(T_{in} - T_w)(x - x_0)k_w}{Dc_v\rho v \left(T_{in} + \left(e^{\frac{k_w(x-x_0)}{Dc_v\rho v}} - 1 \right) T_w \right)}}_{\kappa_{k_w}(q)} \varepsilon_{15} - \underbrace{\frac{(T_{in} - T_w)k_w x}{Dc_v\rho v T(q)} e^{-\frac{k_w(x-x_0)}{Dc_v\rho v}}}_{\kappa_x(q)} \varepsilon_x \\ &\quad + \underbrace{\frac{(T_{in} - T_w)k_w x_0}{Dc_v\rho v T(q)} e^{-\frac{k_w(x-x_0)}{Dc_v\rho v}}}_{\kappa_{x_0}(q)} \varepsilon_{x_0} + O((\Delta q)^2). \end{aligned} \quad (24)$$

We are interested, in whether the relative errors ε_{13} , ε_{14} , ε_{15} , ε_x , and ε_{x_0} in the input parameters are amplified in the relative error for the temperature T . To this end, the nominal values

$$\begin{aligned} D_{nom} &= 1, \\ \rho_{nom} &= 1, \\ v_{nom} &= 10, \\ T_{in_{nom}} &= 293, \\ T_{w_{nom}} &= 283, \\ k_{w_{nom}} &= 0.0341, \\ c_{v_{nom}} &= 1700, \text{ and} \\ x_{0_{nom}} &= 0, \end{aligned} \quad (25)$$

are inserted in the individual relative condition numbers in Eq. (24). With $x_{0_{nom}} = 0$ it holds that $\kappa_{x_0}(q_{nom}) = 0$. The four remaining relative condition numbers are given in

Fig. 3 as a function of the pipeline length $L = x - x_0$. The figure shows that all relative condition numbers remain below one, which means that the relative errors in the input parameters are not amplified. The relative condition numbers κ_{k_w} and κ_x are so small compared with $\kappa_{T_{in}}$ and κ_{T_w} , that they can be neglected.

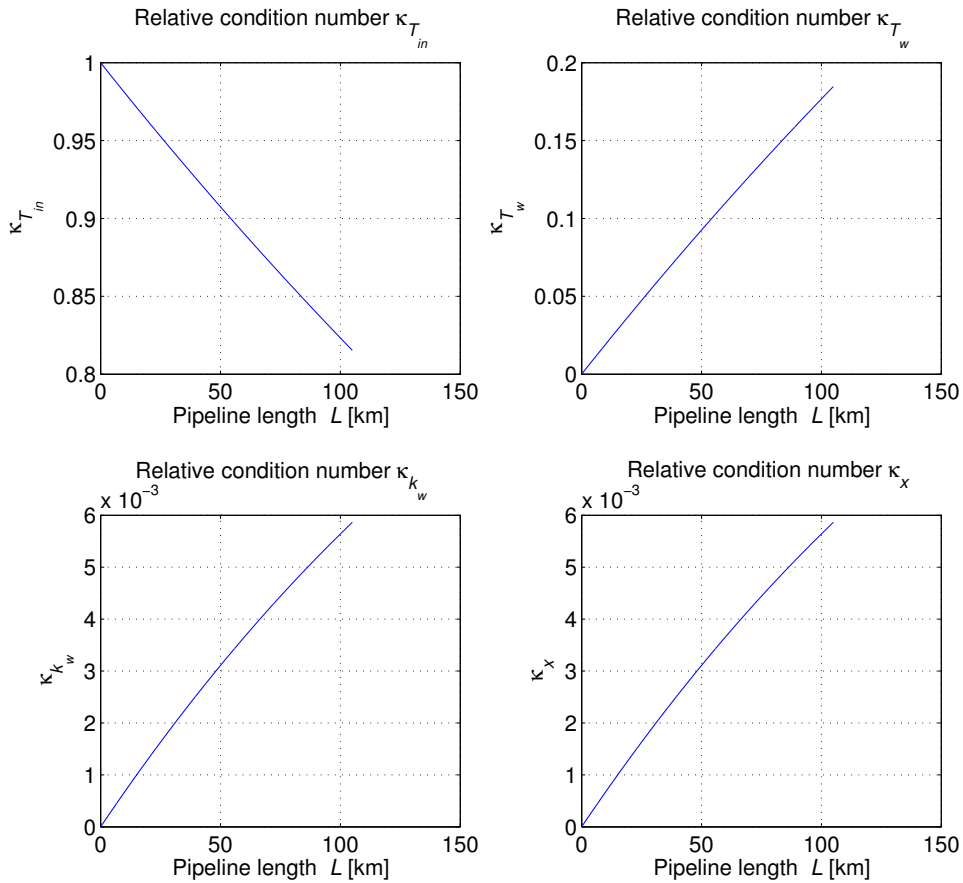


Fig. 3: The individual relative condition numbers $\kappa_{T_{in}}$, κ_{T_w} , κ_{k_w} , and κ_x for the temperature T , considered as a function of the pipeline length $L = x - x_0$.

2.2 Statistical Analysis

A statistical analysis for the algebraic model in Eq. (10) is performed in this section. This analysis is complementary to the theoretical analysis carried out in Sec. 2.1. It aims to statistically validate the theoretical results obtained in Sec. 2.1. This is done by explicitly perturbing the input parameters and calculating the corresponding output parameter values. It gives direct insight in the sensitivity of the output parameters to perturbations in the input parameters. First, in Sec. 2.2.1, the statistical analysis is performed using a Monte Carlo Simulation (MCS). This simulation has the advantage that the accuracy can be arbitrarily increased by enlarging the sample size. However, it has the disadvantage that the sample size should be large to get reliable results, i.e., the computational complexity is high. Second, in Sec. 2.2.2, the statistical analysis is performed using the Univariate Reduced Quadrature (URQ) Method. This method is characterized by a small sample size, together with a fixed accuracy. The small sample size and the corresponding low computational complexity allow us to calculate the sensitivity of the output parameters for many different pipeline lengths.

2.2.1 Monte Carlo Simulation

For this simulation, the input parameters $\mathbf{q} \in \mathbb{R}^n$ are considered to be random variables. The mean $\mu_{\mathbf{q}}$ of these variables is given by the nominal values in Eqs. (20) and (25). The standard deviation $\sigma_{\mathbf{q}}$ of the input parameters is set to 0.5% of the mean, so that for the relative standard deviation (rsd) it holds that $\sigma_{q_i}/\mu_{q_i} = 0.5\%$ for every element q_i of \mathbf{q} . Then, samples are drawn from those distributions. For the sample size N we choose $N = 10^4$. The mean μ_f and variance σ_f^2 of the output parameters \mathbf{f} are approximated using the well-known formulas [3]

$$\mu_{f_{\text{MCS}}} = \frac{1}{N} \sum_{i=1}^N f(\mathbf{q}_i) \quad (26)$$

and

$$\sigma_{f_{\text{MCS}}}^2 = \frac{1}{N-1} \sum_{i=1}^N [f(\mathbf{q}_i) - \mu_{f_{\text{MCS}}}]^2. \quad (27)$$

The error of these approximations is given by [11]

$$|\mu_f - \mu_{f_{\text{MCS}}}| = O(1/\sqrt{N}) \quad \text{and} \quad |\sigma_f^2 - \sigma_{f_{\text{MCS}}}^2| = O(1/\sqrt{N}).$$

So, the accuracy can be arbitrarily increased, although the order of convergence is only 1/2. The sample size depends on the desired accuracy of the output distribution. Note that the error is independent of the problem dimension n , which makes a MCS unaffected by the ‘‘curse of dimensionality’’.

The result of the simulation for the mass flux f_1 in Eq. (11) is given in Fig. 4. It shows that $\mu_{f_1} \approx 10$. The rsd for f_1 , σ_{f_1}/μ_{f_1} , is equal to 0.7%. This corresponds with the theoretical analysis carried out in Sec. 2.1.1, which resulted in a relative error for f_1 that is smaller than or equal to the sum of the relative errors of the input parameters. Indeed, $0.7\% \leq 0.5\% + 0.5\%$.

The result of the MCS for the pressure, Eq. (14), is given in Fig. 5. It shows the output distribution for both normally and uniformly distributed input parameters for several pipeline lengths. There is basically no difference in the rsd of the pressure p between normally and uniformly distributed input parameters. The rsd of p grows quickly with increasing pipeline length L . This corresponds with the analytical analysis in Sec. 2.1.2 together with Fig. 2, where we also found that the relative condition numbers grow quickly with increasing L .

For the temperature T in Eq. (22) the result of the MCS is given in Fig. 6. There is no difference in the rsd of T between normally and uniformly distributed input parameters, although the shape of the output distribution is different. With increasing pipeline length L , the rsd of T decreases slightly. This is in line with the theoretical analysis carried out in Sec. 2.1.3 and with Fig. 3, where we found that all relative condition numbers stay below one for all pipeline lengths, i.e., the relative errors of the input parameters are not amplified.

2.2.2 URQ Method

The URQ method [11] is developed to find an appropriate trade-off between computational complexity and accuracy. Whereas the MCS method in Eqs. (26) and (27) is usually performed with a sample size N of approximately 10^4 , the URQ method only utilizes a sample size of $N = 2n + 1$, where n is the number of input parameters. This

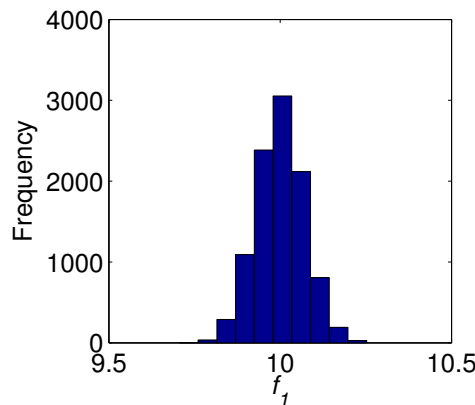


Fig. 4: Result of a MCS for the mass flux f_1 , Eq. (11). The input parameters are normally distributed with a rsd of 0.5%.

makes the URQ method computationally much less expensive than the MCS method, especially for computationally demanding analysis codes, i.e., when the evaluation of $f(\mathbf{q})$ is computationally expensive. The mean μ_f and the variance σ_f^2 of an output parameter f are approximated in the URQ method using the following quadrature formu-

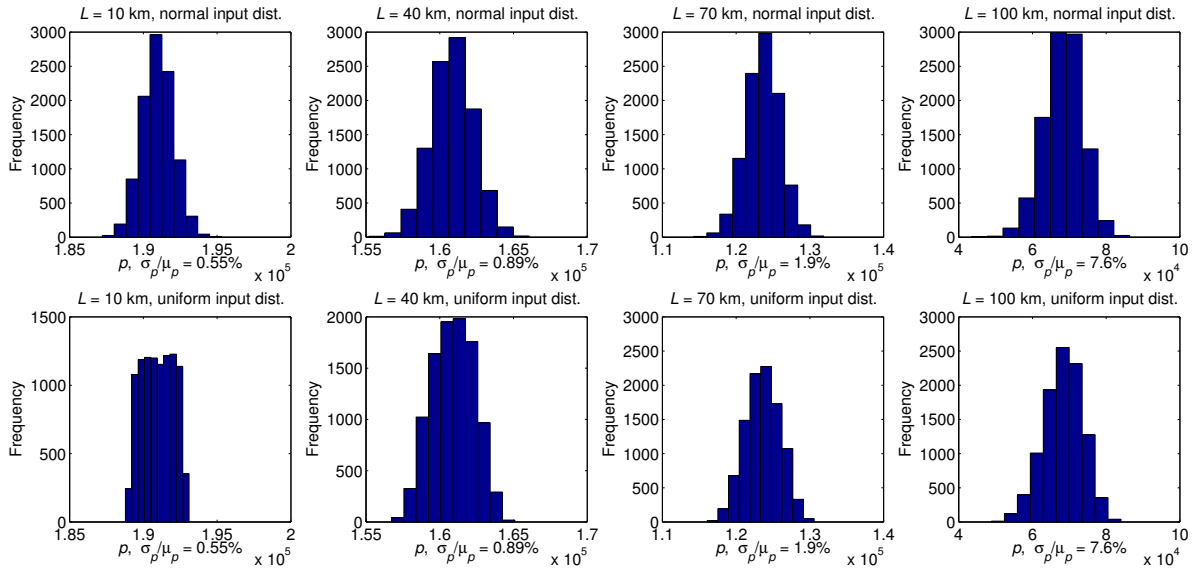


Fig. 5: Result of a MCS for the pressure p , Eq. (14), for different pipeline lengths. The input parameters are either normally or uniformly distributed with a rsd of 0.5%.

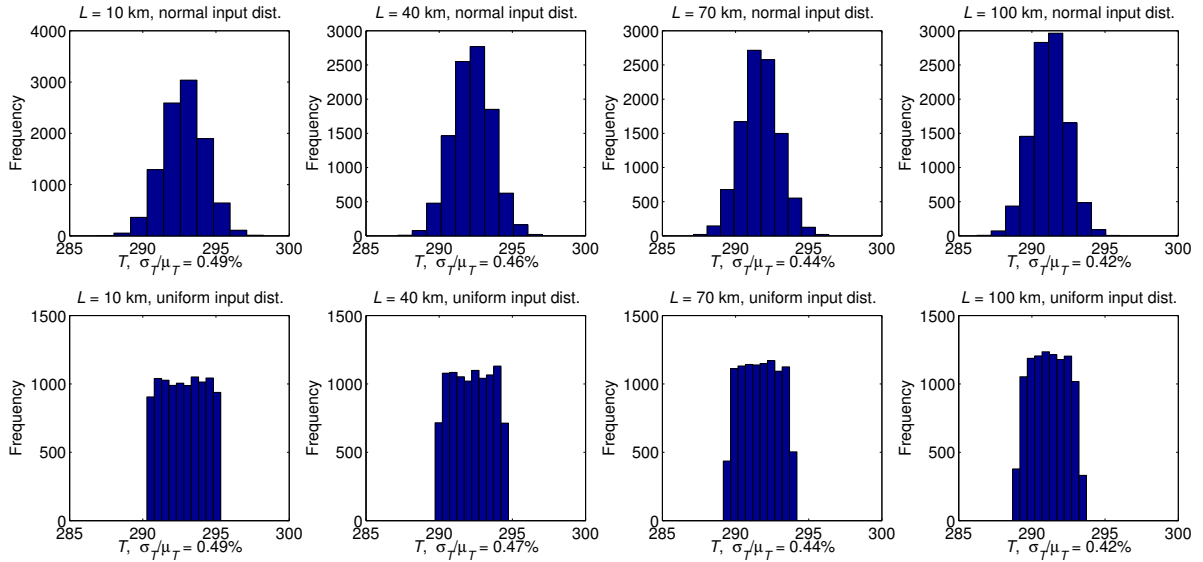


Fig. 6: Result of a MCS for the temperature T , Eq. (22), for different pipeline lengths. The input parameters are either normally or uniformly distributed with a rsd of 0.5%.

las [11]:

$$\mu_{f_{\text{URQ}}}(\boldsymbol{\mu}_q) = W_0 f(\boldsymbol{\mu}_q) + \sum_{i=1}^n W_i \left[\frac{f(\mathbf{q}_i^+)}{h_i^+} - \frac{f(\mathbf{q}_i^-)}{h_i^-} \right] \quad (28)$$

and

$$\sigma_{f_{\text{URQ}}}^2(\boldsymbol{\mu}_q) = \sum_{i=1}^n \left\{ W_i^+ \left[\frac{f(\mathbf{q}_i^+) - f(\boldsymbol{\mu}_q)}{h_i^+} \right]^2 + W_i^- \left[\frac{f(\mathbf{q}_i^-) - f(\boldsymbol{\mu}_q)}{h_i^-} \right]^2 + W_i^\pm \frac{[f(\mathbf{q}_i^+) - f(\boldsymbol{\mu}_q)][f(\mathbf{q}_i^-) - f(\boldsymbol{\mu}_q)]}{h_i^+ h_i^-} \right\}, \quad (29)$$

with appropriately chosen sampling points \mathbf{q}_i , weights W_i , and scaling parameters h_i , which can be found in [11]. The error in these approximations is given by [11]

$$|\mu_f - \mu_{f_{\text{URQ}}}| = O(\sigma_q^4) \quad \text{and} \quad |\sigma_f^2 - \sigma_{f_{\text{URQ}}}^2| = O(\sigma_q^4),$$

where $O(\sigma_q^4)$ denotes all terms of order 4 and higher, i.e., terms proportional to $\sigma_{q_i}^2 \sigma_{q_j}^2$, $\sigma_{q_i}^3 \sigma_{q_j}^2$, etc., for $i, j \in \{1, \dots, n\}$.

This efficient uncertainty propagation technique enables us to calculate the rsd of the pressure p and the temperature T for many different pipeline lengths L . The mean of the remaining input parameters is set to the nominal values in Eqs. (20) and (25). Again, it holds for the rsd $\sigma_{q_i}/\mu_{q_i} = 0.5\%$ for every input parameter q_i of \mathbf{q} . The mass flux f_1 is not considered here, because it is constant with respect to L and can be found in Fig. 4.

The result of this simulation for p and T can be found in Fig. 7. We observe the same behavior as in the MCS in Sec. 2.2.1 and in the theoretical analysis in Sec. 2.1, namely

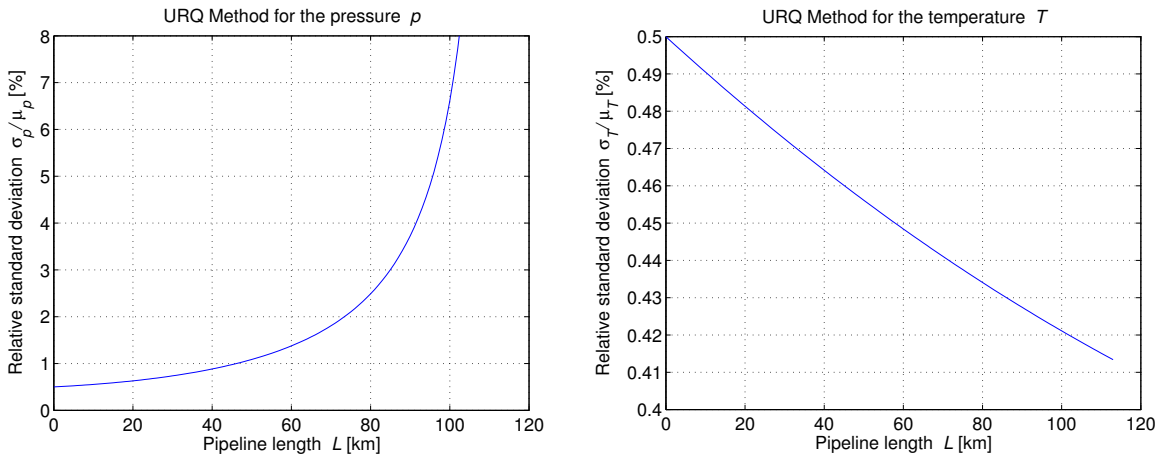


Fig. 7: The relative standard deviation of the pressure (left) and the temperature (right) as a function of the pipeline length. The rsd of the input parameters is 0.5%.

the uncertainty in the pressure p grows quickly for increasing pipeline length L and the uncertainty in the temperature T decreases slightly for increasing L .

2.3 Simplification from Temperature Dependent to Isothermal Algebraic Model

The temperature dependent algebraic model, given by Eqs. (3), (4), and (5), can be simplified by assuming the temperature T to be constant. In this way, the isothermal algebraic model given by Eqs. (3) and (4) is obtained. The first order approximation of the relative error that is made in this simplification is given by Eq. (7), where the temperature T is inserted for f . The vector relative condition number, Eq. (9), of T for the nominal values \mathbf{q}_{nom} in Eq. (25) together with $x_{nom} = 7 \cdot 10^4$ (70 km) is given by

$$\kappa(\mathbf{q}_{nom}) = \begin{bmatrix} \left| \frac{\partial T}{\partial \rho}(\mathbf{q}_{nom}) \frac{\rho}{T(\mathbf{q}_{nom})} \right| \\ \left| \frac{\partial T}{\partial v}(\mathbf{q}_{nom}) \frac{v}{T(\mathbf{q}_{nom})} \right| \\ \left| \frac{\partial T}{\partial D}(\mathbf{q}_{nom}) \frac{D}{T(\mathbf{q}_{nom})} \right| \\ \left| \frac{\partial T}{\partial x}(\mathbf{q}_{nom}) \frac{x}{T(\mathbf{q}_{nom})} \right| \\ \left| \frac{\partial T}{\partial x_0}(\mathbf{q}_{nom}) \frac{x_0}{T(\mathbf{q}_{nom})} \right| \\ \left| \frac{\partial T}{\partial T_{in}}(\mathbf{q}_{nom}) \frac{T_{in}}{T(\mathbf{q}_{nom})} \right| \\ \left| \frac{\partial T}{\partial T_w}(\mathbf{q}_{nom}) \frac{T_w}{T(\mathbf{q}_{nom})} \right| \\ \left| \frac{\partial T}{\partial k_w}(\mathbf{q}_{nom}) \frac{k_w}{T(\mathbf{q}_{nom})} \right| \\ \left| \frac{\partial T}{\partial c_v}(\mathbf{q}_{nom}) \frac{c_v}{T(\mathbf{q}_{nom})} \right| \end{bmatrix}^T = \begin{bmatrix} 0.0042 \\ 0.0042 \\ 0.0042 \\ 0.0042 \\ 0 \\ 0.8729 \\ 0.1271 \\ 0.0042 \\ 0.0042 \end{bmatrix}^T.$$

It follows that only perturbations in the parameter T_{in} create an equivalent relative error in the temperature T . Perturbations in the other input parameters only cause a small relative error in T . This means that if the input temperature T_{in} is not subject to change, the temperature can safely be set constant. If, however, the input temperature changes, for example for different pipelines, the temperature can not be set constant and the temperature dependent algebraic model should be chosen.

We now analyse the case where in the formula for the temperature

$$T(x) = (T_{in} - T_w)e^{-\frac{k_w}{Dc_v\rho v}(x-x_0)} + T_w$$

only the parameter x is variable and the other variables are fixed. We assume that the length of the pipeline L is 100 km and that $x_0 = 0$. The maximum absolute error E_{abs}

that is made when the temperature is set constant is then given by

$$\max_{x \in [0, 100 \text{ km}]} E_{abs} = \max_{x \in [0, 100 \text{ km}]} |T - T(x)| = \max_{x \in [0, 100 \text{ km}]} |T - (T_{in} - T_w)e^{-\frac{k_w}{Dc_v\rho v}(x-x_0)} - T_w|. \quad (30)$$

The maximum relative error E_{rel} that is made when T is set constant is given by

$$\max_{x \in [0, 100 \text{ km}]} E_{rel} = \max_{x \in [0, 100 \text{ km}]} \frac{|T - T(x)|}{|T(x)|} = \max_{x \in [0, 100 \text{ km}]} \frac{|T - (T_{in} - T_w)e^{-\frac{k_w}{Dc_v\rho v}(x-x_0)} - T_w|}{|(T_{in} - T_w)e^{-\frac{k_w}{Dc_v\rho v}(x-x_0)} + T_w|}. \quad (31)$$

One possibility to set the temperature constant would be to measure the temperature at the beginning and at the end of the pipeline and to take the average value, i.e.,

$$T = \frac{T(0) + T(100 \text{ km})}{2}.$$

Then, the graphs for the variable and the constant temperature for the nominal values q_{nom} in Eq. (25) are given in Fig. 8. For these nominal values the maximum absolute error in Eq. (30) is $E_{abs} = 0.909$ and the maximum relative error in Eq. (31) is $E_{rel} = 0.0031$. This is a small relative error, such that in this case the temperature can safely be set constant.

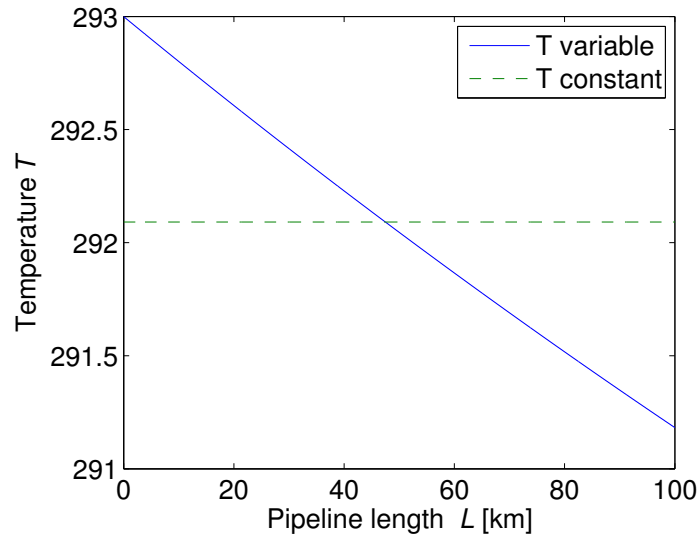


Fig. 8: Graphs for variable temperature with the nominal values in Eq. (25) and for constant temperature as the average of $T(0)$ and $T(100 \text{ km})$.

3 Conclusion

The error analysis for the mass flux results in an error that is smaller than or equal to the sum of the errors of the two input parameters. Both the theoretical and the statistical analysis for the pressure show that the error grows quickly with increasing pipeline length, from which it is concluded that the algebraic model can only be used safely for pipelines up to 60 km length. On the other hand, the error in the temperature decreases slightly with increasing pipeline length.

Finally, it is shown in this work that only if the pipeline input temperature is not subject to change, the temperature can safely be set constant and the isothermal algebraic model can be used. Otherwise, the temperature dependent algebraic model should be used to simulate the gas flow.

Acknowledgements

The authors would like to thank both Dr. A. Międlar for the inspiring discussions and the Deutsche Forschungsgemeinschaft for their support within Projekt B03 in the Sonderforschungsbereich / Transregio 154 *Mathematical Modelling, Simulation and Optimization using the Example of Gas Networks*.

References

- [1] M. Bollhöfer and V. Mehrmann. *Numerische Mathematik: Eine Projektorientierte Einführung Für Ingenieure, Mathematiker und Naturwissenschaftler*. Vieweg Studium; Grundkurs Mathematik. Vieweg+Teubner Verlag, 2004.
- [2] J. Brouwer, I. Gasser, and M. Herty. Gas pipeline models revisited: Model hierarchies, nonisothermal models, and simulations of networks. *Multiscale Modeling & Simulation*, 9(2):601–623, 2011.
- [3] F.M. Dekking, C. Kraaikamp, H.P. Lopuhaä, and L.E. Meester. *A Modern Introduction to Probability and Statistics: Understanding Why and How*. Springer Texts in Statistics. Springer London, 2010.
- [4] P. Domschke, O. Kolb, and J. Lang. Adjoint-based control of model and discretisation errors for gas and water supply networks. In X. Yang and S. Koziel, editors, *Computational Optimization and Applications in Engineering and Industry*, pages 1–17. Springer, 2011.
- [5] P. Domschke, O. Kolb, and J. Lang. Adjoint-based control of model and discretisation errors for gas flow in networks. *Int. J. Mathematical Modelling and Numerical Optimisation*, 2(2):175–193, 2011.
- [6] Energy Consumption in Germany. <http://www.bmwi.de/BMWi/Redaktion/Binaer/Energiedaten/energiegewinnung-und-energieverbrauch2-primaerenergieverbrauch.xls>. Accessed: 2014-11-05.
- [7] Gas pipelines in Europe. [https://www.bdew.de/internet.nsf/res/EM_2012E_S_24-25.jpg/\\$file/EM_2012E_S_24-25.jpg](https://www.bdew.de/internet.nsf/res/EM_2012E_S_24-25.jpg/$file/EM_2012E_S_24-25.jpg). Accessed: 2014-11-05.
- [8] N.J. Higham. *Accuracy and Stability of Numerical Algorithms*. Society for Industrial and Applied Mathematics, 1996.
- [9] M. Konstantinov, D.W. Gu, V. Mehrmann, and P. Petkov. *Perturbation Theory for Matrix Equations*. Studies in Computational Mathematics. Elsevier Science, 2003.
- [10] R. Le Veque. *Finite Volume Methods for Hyperbolic Problems*. Cambridge Texts in Applied Mathematics, Cambridge University Press, 2002.
- [11] M. Padulo, M. S. Campobasso, and M. D. Guenov. Novel Uncertainty Propagation Method for Robust Aerodynamic Design. *AIAA Journal*, 49(3):530–543, 2011.
- [12] J.R. Rice. *Numerical Methods, Software, and Analysis*. Academic Press, 1993.